

## CARBON FROM UBANGI—A MICROSTRUCTURAL STUDY

LUCIEN F. TRUEB, *Metallurgy and Materials Science Division,  
Denver Research Institute, University of Denver,  
Denver, Colorado 80210*

AND

E. CHRISTIAAN DE WYS, *Dept. of Geosciences, Texas Tech University,  
Lubbock, Texas 79406*

### ABSTRACT

Carbon originating from Ubangi (Central African Republic) is a dark-colored variety of polycrystalline diamond resembling Brazilian carbonado. It consists of a porous matrix of randomly oriented, mainly anhedral crystallites ranging from 0.5 to 20  $\mu\text{m}$  which often encloses well-formed octahedral and cubic diamonds with an edge length of up to 500  $\mu\text{m}$ . The pores contain inclusions of florencite and small amounts of other minerals which are usually associated with diamond in alluvial deposits.

### INTRODUCTION

Until the beginning of this century, the state of Bahia, Brazil was the sole commercial source of black diamond, the so-called carbonado. Because of its polycrystalline habit, this material is extremely tough and is still much in demand for use in drill bits designed to pierce the hardest types of rock. As the Brazilian deposits were being played out at the beginning of this century, the price of carbonado rose dramatically, but this development was completely reversed around 1925 when the rich Central African deposits were put into production. Today, only a few thousand carats of drilling grade carbonado are mined in Brazil each year, most of the demand for this type of diamond being covered by carbon from the Ubangi area in the Central African Republic.

Diamond dealers usually reserve the term carbonado for stones of Brazilian origin, while the African variety is designated as carbon. Because it appears to be well established, this somewhat unfortunate nomenclature will be used throughout this paper. It should thus be kept in mind that in the present instance the term carbon refers specifically to the black polycrystalline diamond from central Africa.

Diamond is found throughout the territory of the Central African Republic, but mining is concentrated in two areas: Berbezati, Carnot, Nola in the West (West Ubangi), and Ouadda, N'Dele in the North-East (East Ubangi), the two centers being some 600 km apart. In the East, the carbons are usually small and form only 6 to 7 percent of the total diamond production, while in the West they are quite large and their proportion reaches up to 30 percent. In this latter area, large, white, monocrystalline diamonds are relatively rare; this negative correlation

has been explained by the assumption that carbon was formed in higher areas of its still unknown matrix where rapid decompression and cooling may occur, resulting in a high nucleation rate and the growth of many small, imperfect crystallites. Since the Ubangi diamond fields are strictly sedimentary, carbon would be most abundant in the stratigraphically lowest deposits formed during the early stages of erosion. Conversely, large monocrystalline diamond the growth of which needs a long time and steady pressure-temperature conditions would be found in the lower parts of the matrix which are the last to erode and thus deposited in the youngest layers of the sediment. (Bardet, 1959, private communication). It must be noted, however, that the central African diamond fields consist of cretaceous alluvial sandstones and conglomerates; despite a great amount of prospecting and geological surveying, no kimberlite pipes nor any kimerlitic mineral have ever been found in Central Africa.

Aside from the newly-discovered fields in the USSR (Central Ural and Yakutiya), black diamond is found exclusively in Brazil and Central Africa, which has led to the speculation that these latter deposits may have a common origin. In fact, the two locations would have been separated by less than 1300 km before the assumed break-up of Pangea. However, despite some microstructural similarities between carbonado and carbon to be described below, this theory cannot be unequivocally corroborated by the present investigation.

Carbon is found in irregularly-shaped lumps with an average diameter of 8 to 12 mm (approximately 20 carats), although much larger stones up to several hundred carat are by no means rare. The largest known Central African stone weighs 740.25 carats and is exhibited at the Smithsonian Institution in Washington D.C.

To our knowledge, most published microstructural work concerning black diamond was performed on Brazilian samples; reviews of this literature have been recently published (Trueb and Buttermann, 1969; Trueb and de Wys, 1969). Aside from a report in book-form which deals mainly with the geography and geology of Ubangi diamond fields (Bruet, 1952), carbon from Ubangi has received very little attention so far, despite its easy availability and the mystery surrounding its origin. These reasons prompted us to undertake the present investigation.

#### EXPERIMENTAL RESULTS AND DISCUSSION

All the results reported here were obtained on a series of ten carbons from Ubangi weighing between 4.0 and 5.4 carat; they were chosen randomly from a 20,000 carat batch. It could not be ascertained whether the samples originated from East or West Ubangi.

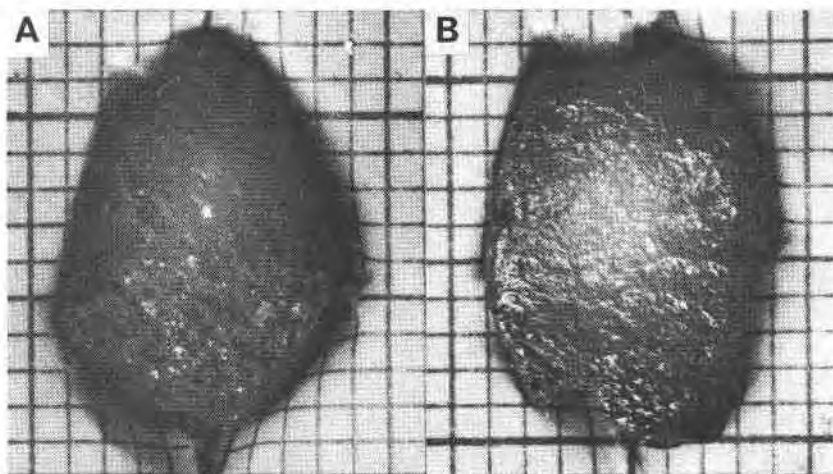


FIG. 1. Two samples of carbon from Ubangi, as received.  
Background subdivisions: 1 mm.

The samples were uniformly dark-gray to black and were either dull or lustrous, depending on the amount of polishing they received after erosion and subsequent transport by the drainage system. Also, some of the samples were obviously fragments of larger stones, while others were in the form of bean-shaped, well-rounded pebbles. The surfaces were usually pitted and contained variable numbers of irregularly-shaped pores with a diameter of 100 to 300  $\mu\text{m}$ , often filled with reddish-brown to yellowish-white impurities. Figure 1 shows the surface structure of two representative specimens.

The densities as determined by a precision pycnometric method varied from 3.176 to 3.301, the average value being 3.292  $\text{g}\cdot\text{cm}^{-3}$ . Since the density of pure white diamond is 3.511  $\text{g}\cdot\text{cm}^{-3}$ , the average porosity of the samples was 6.2 percent.

*Inclusions.* The distribution of the inclusions was determined by contact X-ray radiography. For this purpose, the carbons were tied to a piece of KODAK high resolution plate by means of "Saran Wrap" and exposed for a few seconds to nickel-filtered copper radiation. A modified Debye-Scherrer camera operated without collimators and provided with a pinhole aperture at the incident beam porthole was used. Photographic enlargements were prepared directly from the resulting exposures and two examples are given in Figure 2. Sample A in Fig. 2 contained a relatively large amount of inclusions or aggregates thereof, the size of which varied from 40 to 500  $\mu\text{m}$ . Sample B contained considerably

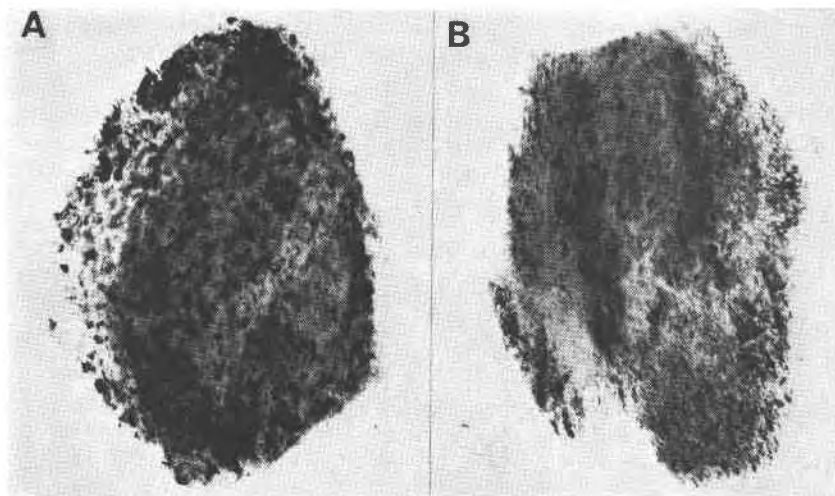


FIG. 2. X-ray contact radiographs of the two carbons shown in Fig. 2. (Magnification 15% higher). The black spots are inclusions.

fewer highly absorbing inclusions and their average diameter was approximately  $60 \mu\text{m}$ . In the latter instance several areas with a preferred orientation of the inclusions could be observed, which may be due to a more or less parallel alignment of the pores; this effect has already been noted in carbonado, where it occurs to a considerable extent (Trueb and Butterman, 1969).

*Fracture Surfaces.* In order to investigate the microstructural features of the bulk of the specimens, fresh fracture surfaces were produced by carefully crushing the carbons in a large vise. Considerable force was required to that effect, and the jaws of the vise were usually dented extensively before fracture occurred with a loud report. The light-gray fractured interfaces were then examined by light-optical, scanning and transmission electron microscopy.

Figure 3 shows the appearance of a fracture interface of one of the more porous specimens ( $\rho = 3.267 \text{ g}\cdot\text{cm}^{-3}$ ) in the light microscope at low magnification. The individual crystallites cannot be resolved very clearly in this instance since the irregularly fractured interfaces emit a great many specular reflections. However, the presence of a considerable number of usually elongated pores is clearly evident. Furthermore, close examination of the pores showed that they contained inclusions which often filled them out completely, which is difficult to recognize in black and white photographs.

Figure 4 is a scanning electron micrograph showing the fracture interface of a relatively pore-free specimen ( $\rho = 3.335 \text{ g}\cdot\text{cm}^{-3}$ ). At this magnification, the diamond crystallites appear to be mainly anhedral, and their size ranges from 2 to 40  $\mu\text{m}$ , the main fraction having a diameter of 5 to 10  $\mu\text{m}$ .

Figure 5 shows rather large monocrystals distributed within the matrix of 10  $\mu\text{m}$  crystallites. This feature, while not being unusual, was

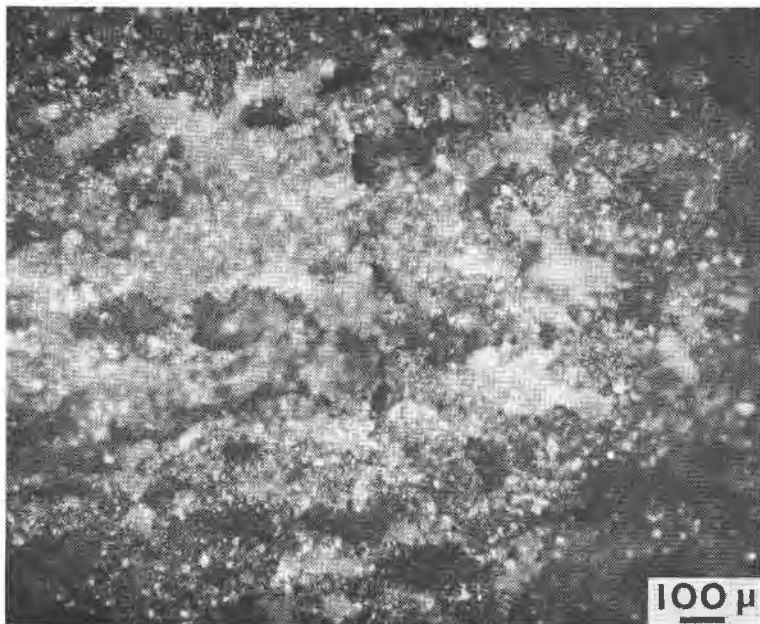


FIG. 3. Fracture interface of Ubangi carbon showing elongated pores and intergranular inclusions.

observed only in part of the carbon samples. In this instance the edge length was of the order of 250  $\mu\text{m}$ . This crystal was fractured during crushing and only its cross-section can be seen in Figure 5; it exhibits the characteristic pattern of steps which appears whenever diamond breaks under the effect of stresses that are not parallel to a cleavage plane. At the lower right in Figure 5, a smaller, well-preserved octahedron with an edge length of 100  $\mu\text{m}$  (arrow) can be seen with two  $\{111\}$  planes emerging from the polycrystalline matrix. These relatively large crystals usually appeared in clusters and their surfaces were often peeled out of the surrounding material during crushing, which indicates relatively poor adhesion to the matrix. Carbons with inclusions of large octahedral and sometimes cubic diamond crystals were thus presumably

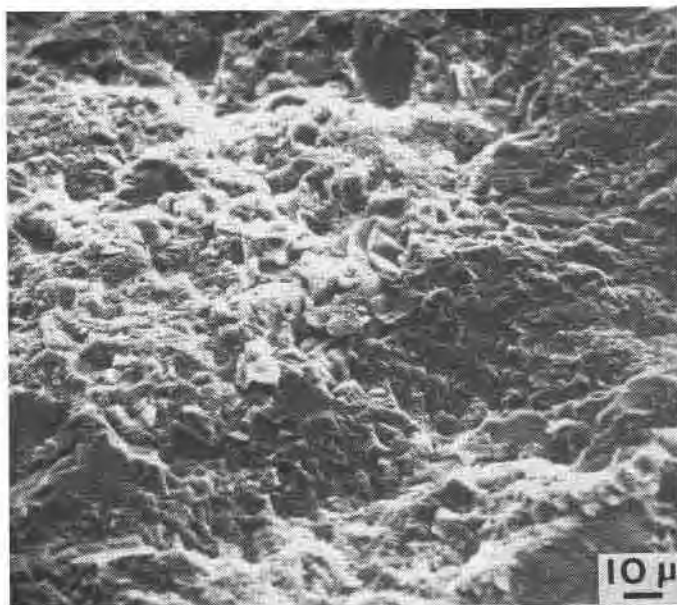


FIG. 4. Scanning electron micrograph of fracture interface.

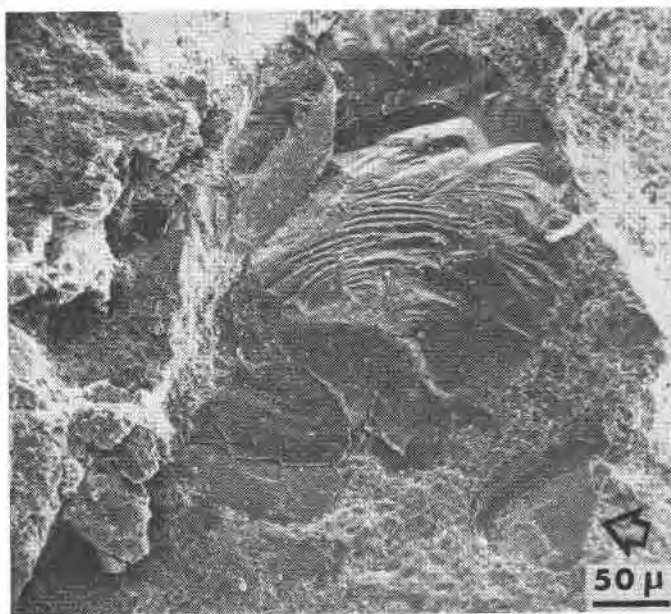


FIG. 5. Scanning electron micrograph showing cross-section of large diamond crystal (center) and smaller octahedron (lower right, arrow) embedded in the polycrystalline matrix.

formed in two stages: a slow nucleation and growth process leading to small but near-perfect crystals, followed by the formation of a matrix of mainly anhedral, small and disordered crystallites which appeared under conditions favoring a high nucleation rate, most likely a rapid release of pressure due to a seismic or volcanic process.

In order to gain more detailed information about the size, shape and fracture mode of the diamond crystallites in carbon, freshly fractured interfaces were replicated by means of a two-stage cellulose acetate/carbon method with platinum palladium pre-shadowing. These replicas were examined by electron microscopy; Figures 6 and 7 are representative micrographs depicting the substructure of the polycrystalline matrix. Figure 6 shows densely packed and interlocked crystallites the size of which varies from less than 1 to 20  $\mu\text{m}$ . While the larger crystallites appeared to be mainly anhedral, octahedra and deformed octahedra were often observed within the 1 to 4  $\mu\text{m}$  range. Both the intergranular and transgranular fracture mode were apparent, the latter usually involving  $\{111\}$  cleavage which leads either to very smooth surfaces or



FIG. 6. Electron micrograph of fracture interface of Ubangi carbon, showing both intergranular and transgranular fracture. (Replica)

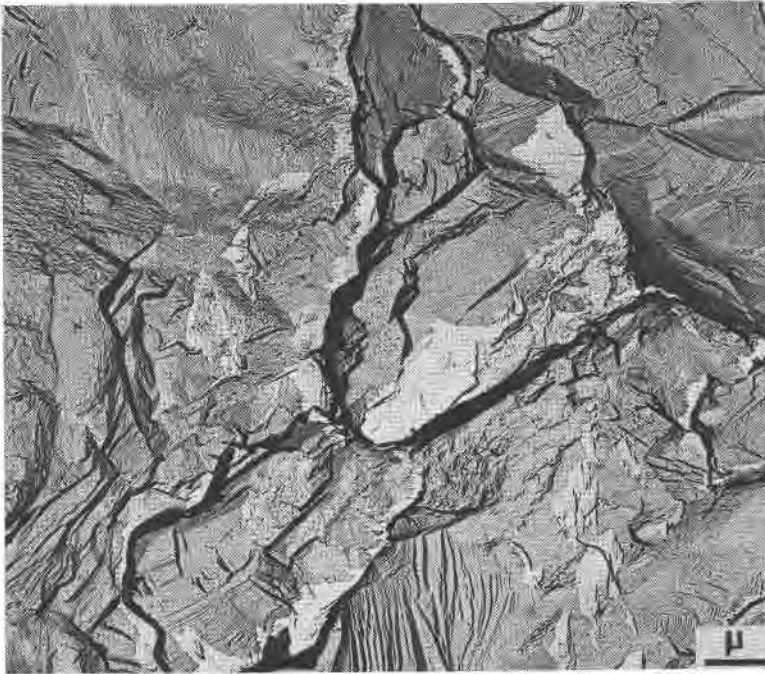


FIG. 7. Electron micrograph of fracture interface; the individual crystallites are outlined by intergranular cracks or voids. (Replica)

patterns of steps with alternating directions, depending on the orientation of the crystallites with respect to the stress applied when breaking the specimen.

Intergranular fracture exposes the true crystallite boundaries which invariably exhibit a mottled pattern (Fig. 6, top right). Close examination revealed that this mottling consisted of large numbers of minute octahedra ranging from 200 to 1500 Å and arranged in preferred orientation on each crystal facet. Analysis of the shadow direction on the replica showed that all these octahedra were depressions on the outer surface of the crystallites. They may thus be negative crystals formed under the effect of gases or fluids (*e.g.*, carbon dioxide which is often found as an inclusion in monocrystalline diamond) entrapped under high pressure between two adjacent boundaries.

Similar features can also be observed in Figure 7 in which a majority of the crystallites are outlined by relatively broad black ribbons. This is an artifact due to the intrusion of replicating plastic between crystallites, but indicates the presence of interstices or cracks at the grain boundaries.





FIG. 8. Fracture interface of 250  $\mu\text{m}$  diamond crystal embedded in the polycrystalline matrix. (Replica)

Most of the cleaved surfaces were practically featureless, the main imperfections being series of lens-shaped voids with a length of 0.2 to 0.3  $\mu\text{m}$  and a width of 200 to 600  $\text{\AA}$  appearing in parallel arrays and running in one or two definite directions. (Fig. 7, upper left).

A somewhat unusual fracture pattern of one of the large diamond crystals embedded in the polycrystalline matrix is shown in Figure 8. In this instance the stress applied to fracture the stone must have been oriented rather exactly in the  $[100]$  direction, which resulted in localized symmetrical cleavage on  $\{111\}$  planes forming a pattern of similarly oriented octahedra extending over the entire fracture surface.

Although the crystallites themselves apparently contain small numbers of more or less spheroidal inclusions, the bulk of the inclusions were found either within pores or along grain boundaries where they cause a partial coating of the diamond crystallites. Figure 9 shows that the inclusions apparently seeped into the sample through intergranular gaps, forming irregular patterns of more or less aggregated 0.1 to 0.5  $\mu\text{m}$  diameter hexagonal platelets. No satisfactory extraction replicas were obtained of such surfaces, so that the identification of the platelets

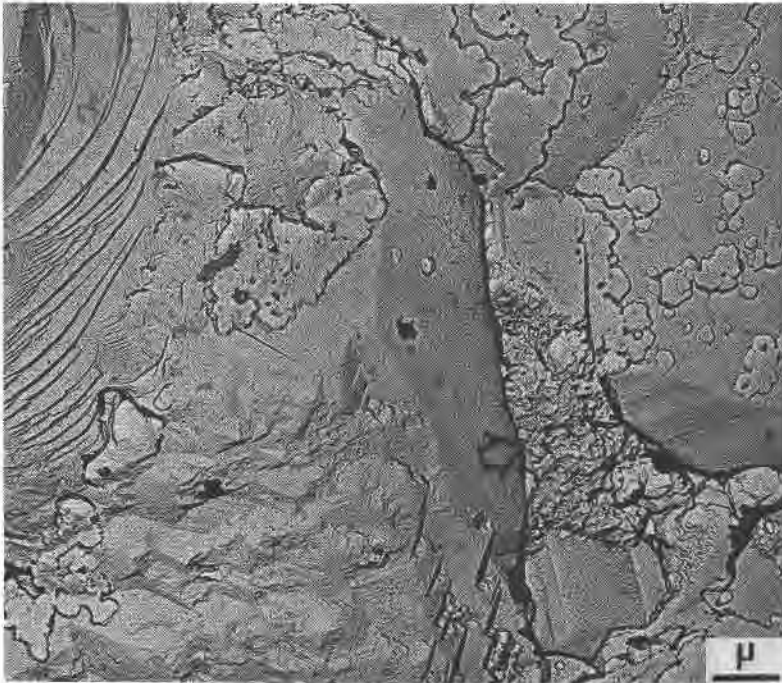


Fig. 9. Fracture interface of Ubangi carbon showing small pore filled with foreign phase (arrow) and platelet-shaped inclusions which seeped into the intergranular voids. (Replica)

by selected area electron diffraction was not possible. However, their geometry suggests that they consist of florencite, the most abundant inclusion in the carbons as reported below.

*Defects Within Diamond Crystallites.* In order to investigate the defects and possible microinclusions within the diamond crystallites themselves, the smallest fragments obtained by crushing carbons were dispersed on specimen support grids coated with a film of amorphous carbon and examined by transmission electron microscopy. Figure 10 shows several concentric dislocation loops in what appears to be a Frank-Read source: a dislocation helix and two isolated dislocations bowing out from one of the edges of the crystallite are also observed. The dislocation density determined from a series of micrographs similar to Figure 10 by means of a grid-intercept method (KEH, 1960) was  $10^8$  to  $10^{10}$   $\text{cm}^{-2}$ , the samples being tilted in the electron microscope for maximum dislocation contrast. Although at least part of these defects were presumably produced during crushing, the relatively high density of dislocations tends to indi-

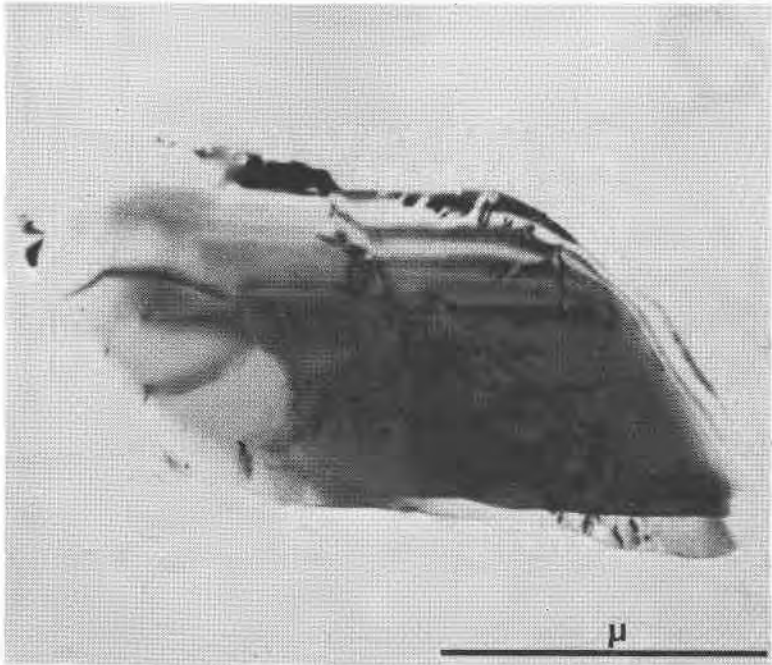


FIG. 10. Transmission electron micrograph of carbon fragment showing dislocations and dislocation loops (center).

cate a significant level of residual stress. This is not unexpected since the crystallites are believed to have grown under conditions well above equilibrium, resulting in rapid nucleation. These observations were further corroborated by electron spin resonance measurements of powdered samples which had been boiled for at least 1 hr in hydrofluoric acid to remove all inclusions. A singlet signal was obtained in the position characteristic for free electrons, and the concentration of free electrons was found to be approximately  $2.6 \times 10^{17}$ , which compares with a published value of  $6.6 \times 10^{17}$  for Brazilian carbonado (Mears and Bowman, 1966). Because of differences in the particle size distribution and the resulting packing density in the specimen holder, these values are prone to significant errors; however, a direct qualitative comparison confirmed that the free electron density of Brazilian material is significantly higher than that of the Ubangi variety.

Other types of lattice defects which were occasionally observed in fragments of carbon were dislocation loops resulting presumably from the collapse of vacancy discs, and elongated dislocation dipoles (Figures 11 and 12) which are commonly found in monocrystalline diamonds and

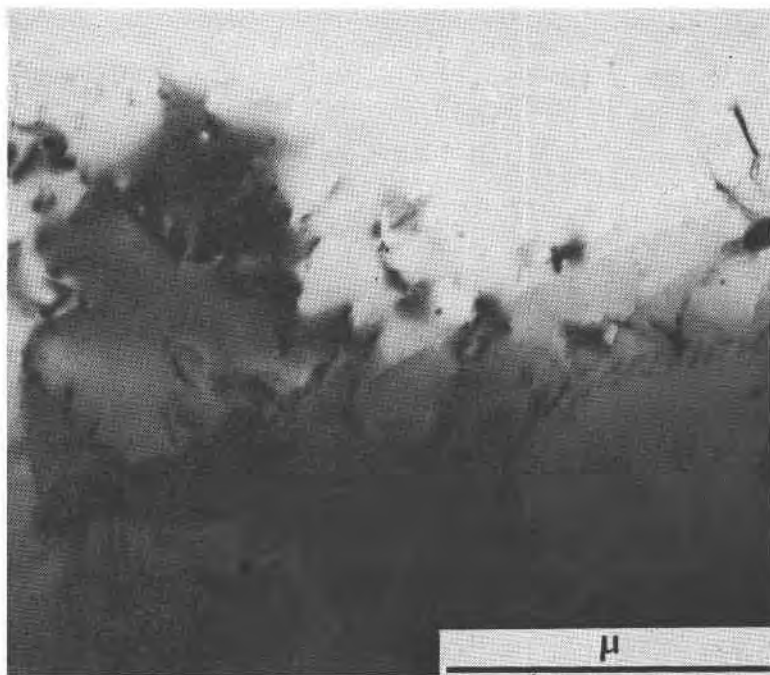


FIG. 11. Transmission electron micrograph showing dislocation loops and helices.

are assumed to be caused by high-temperature motion of screw dislocation containing long jogs (Evans and Phaal, 1962). Although a number of fragments in (100) orientation were carefully examined, the characteristic defect patterns indicating the presence of nitrogen platelets as described by Evans and Phaal (1962) could not be observed. From this point of view, the crystallites forming the carbons can be classified as Type II, although no spectroscopic data are available to corroborate this point.

Figure 12 and many other fragments of carbon that were examined, showed evidence that they contained inclusions, mainly in the form of hexagonal or rectangular particles. However, such evidence alone is not sufficient to decide whether a given suspected inclusion is truly situated within a crystallite or simply happens to be a fragment adhering to one of its surfaces. For this reason, the samples were tilted in the electron microscope until a set of extinction fringes appeared. Only in the instance of true inclusions will a break in the fringe pattern occur; particles adhering to a surface have no effect on the fringes. By means of this method, it was determined that the great majority of suspected inclu-

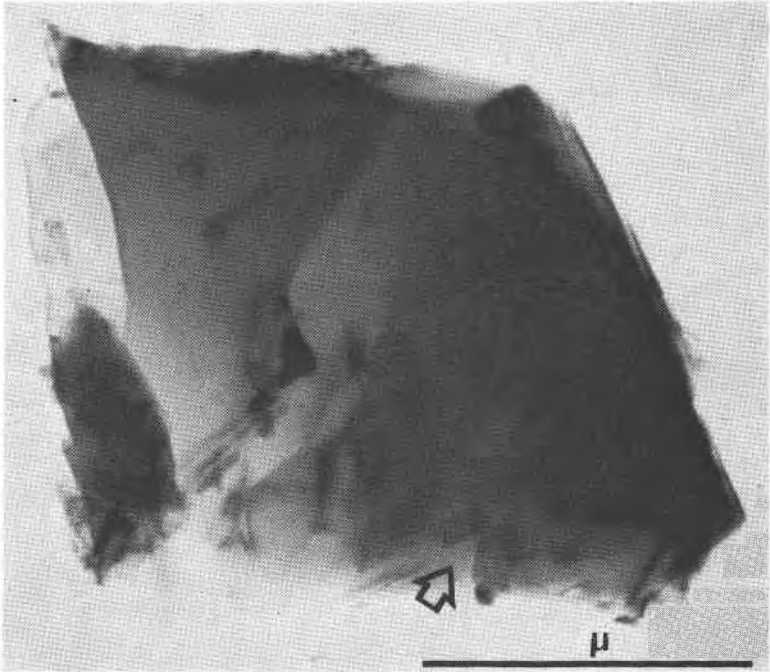


FIG. 12. Transmission electron micrograph showing dislocation dipoles and suspected inclusions.

sions did not pass the test, and only very few true inclusions were observed. This scarcity confirms the result of the study by replication reported above. The diameter of the inclusions observed by transmission electron microscopy was usually below  $500 \text{ \AA}$ , which precluded their identification by selected area diffraction.

*Amount and Composition of Impurities.* The above findings further confirm previous evidence that the majority of the impurities found in carbon is confined to pores, cracks and intergranular interstices. In order to determine the total amount of these impurities, a series of fragments of carbon weighing 0.5 to 1 carat were heated in air at  $1100^{\circ}\text{C}$  for 2 to 3 hr. This caused total combustion of the diamond, the residue consisting of sponge-like skeletal polycrystalline structures ranging from yellowish to brown-gray, still assuming the original shape of the carbon fragments, and small yellowish-white single crystals with an edge length varying between 10 and  $30 \mu\text{m}$ . The weight of this ash was used to determine the percentage value of inclusions which scattered between 1.7 and 3.6 percent, the average being 2.5 percent.

TABLE 1

Elemental Composition of Ubangi Carbon Ash after Combustion  
at 1100°C

<u>Type of Ash Particle</u>	Elemental Constituents
	(Major Elements Underlined, Traces in Parentheses)
White skeleton	<u>Al</u> , <u>Si</u> , P, S, <u>Ca</u> , Fe, <u>La</u> , Ce (Zn, Y, Pr, Nd)
Yellow skeleton	Al, Si, P, <u>Ti</u> , <u>Ca</u> , Ni, La, <u>Ce</u> , Nd, Ba (Si, S, Fe)
Dark-brown skeleton	Al, Ti, <u>Fe</u> , Ni, Ce, Nd (Si, Ca, Cr, La)
Yellowish-white crystallites	<u>Si</u> , P, Ca, Fe, La, Ce, Pr (Al, Ti)

The elemental constituents of the ash particles were determined by electron probe microanalysis. The results are listed in Table 1 and are identical to the elemental compositions obtained for inclusions that were directly extracted from the carbon specimens as described in the next paragraph. Because of possible modifications of the minerals during combustion and microscopic evidence that the ash particles consisted of complex mixtures, only a cursory identification by powder X-ray diffraction was conducted in this instance. It showed that the main constituents of the skeletal fraction was florencite with variable amounts of magnetite, rutile, ilmenite, akermanite, and gehlenite. The small single crystals consisted of monazite and quartz.

In order to obtain a more detailed, localized and nondestructive analysis of the impurities in carbon, inclusions were extracted individually under a binocular microscope by means of a fine needle, both from the outside of the stones and from freshly fractured interfaces. In this instance, the identification proceeded by combining electron probe microanalysis with X-ray diffraction and in some instances electron diffraction and polarization microscopy. The results are listed in Table 2 and show that the predominating inclusion was the rare-earth phosphate florencite which, besides cerium, contained easily detectable amounts of lanthanum, praseodymium, neodymium, and samarium.

The presence of rare earths in carbon is of special interest since they have been detected in diamond-bearing alluvial sediments in Brazil

TABLE 2

External Inclusions in Ubangi Carbons  
(removed from outside pores)

Mineral	Composition
Akermanite-gehlenite	$\text{Ca}_2\text{Al}_2\text{SiO}_7\text{-Ca}_2\text{MgSi}_2\text{O}_7$
aluminian serpentine	$5\text{MgO}\cdot\text{Al}_2\text{O}_3\cdot 3\text{SiO}_2\cdot 4\text{H}_2\text{O}$
Florencite	$(\text{Ce,La,Pr,Nd,Sm})\text{Al}_3(\text{PO}_4)_2(\text{OH})_6$
Hisingerite	$(\text{Fe}_{1.53}^{3+}\text{Mg}_{0.48}\text{Fe}_{0.17}^{2+})(\text{Si}_{3.03}\text{Fe}_{0.27}^{3+}\text{Al}_{0.2})_{10}$
Ilmenite	$\text{FeO}\cdot\text{TiO}_2$
Kaolinite	$\text{Al}_2\text{Si}_2\text{O}_5(\text{OH})_2$
Pyrophyllite	$\text{Al}_2\text{O}_3\cdot 4\text{SiO}_2\cdot \text{H}_2\text{O}$
Quartz	$\text{SiO}_2$
Rutile	$\text{TiO}_2$
Weinschenkite (churchite) (Y,Er,La,Nd,Ce)	$2\text{O}_3\cdot \text{P}_2\text{O}_5\cdot 4\text{H}_2\text{O}$

Internal Inclusions in Ubangi Carbons  
(removed from freshly fractured interfaces)

Mineral	Composition
Aluminian serpentine	$5\text{MgO}\cdot\text{Al}_2\text{O}_3\cdot 3\text{SiO}_2\cdot 4\text{H}_2\text{O}$
High-Al chlorite (amesite?)	$4\text{MgO}\cdot 2\text{Al}_2\text{O}_3\cdot 2\text{SiO}_2\cdot 4\text{H}_2\text{O}$
Chromite	$\text{FeO}\cdot\text{Cr}_2\text{O}_3$
Florencite	$(\text{Ce,La,Pr,Nd,Sm})\text{Al}_3(\text{PO}_4)_2(\text{OH})_6$
Ilmenite	$\text{FeO}\cdot\text{TiO}_2$
Magnetite	$\text{Fe}_3\text{O}_4$
Perovskite	$\text{CaO}\cdot\text{TiO}_2$
Quartz	$\text{SiO}_2$
Olivine	$(\text{Fe, Mg})_2\text{SiO}_4$
Rutile	$\text{TiO}_2$

(the so-called favas), the origin of which has not yet been determined. It is worth noticing in this connection that rare earths also occur in kimberlites; more particularly, it has been found that the kimberlites in Yakutiya are typified by an unusually high cerium content by com-

parison with the lithosphere in general and many magmatic rocks (Bardet 1969). This point is thus confirmed by the present investigation. Also, the yellowish gravel (so-called feoes) cited by Bruet (1952) as typically associated with central African diamond and assumed by the above author to be a phosphate is very likely to be florencite and thus closely related to the Brazilian favas. The presence of florencite but the absence of allanite found in Brazilian carbonado (Trueb and de Wys, 1969) deserves some attention. Allanite is a typical accessory mineral in deep-seated igneous rocks where the temperature conditions have been such as to allow a stable epidote type structure. The occurrence of florencite which is closely related to the alunite group, tends to indicate an association with an acid type volcanic rock subjected to sulfuric acid solution or vapors. Such conditions are typically those of the high pressures and high temperatures which are characteristic of fumaroles. The occurrence of Weinschenkite which is often associated with gypsum in volcanic regions, is indicative of the replacement of calcium by rare earths in a magmatic residual.

Perovskite has not been previously detected as an inclusion in monocrystalline diamond. According to Bardet (1970) citing the theories of Milashev, it is considered as an inhibitor for diamond formation in kimberlites. Whether this point is also related to the scarcity of good monocrystalline diamonds in deposits rich in carbon remains an open question.

The occurrence of olivine, ilmenite, rutile, magnetite, chromite, and the mellilites indicates a basic hypo to mesothermal type of intrusive. Pyrophyllite is typical of schistose rocks and is also found in the Minas Geraes area of Brazil in foliated masses of great extent. Finally, the occurrence of kaolinite and hisingerite is probably indicative of secondary alteration. It is worth noticing that rutile, magnetite, quartz, and ilmenite are cited by Bruet (1952) as being among the typical satellites of diamond, *i.e.* these minerals are invariably associated with diamond in sedimentary deposits formed by multiple-stage erosion and concentration of heavy components.

The presence of graphite as an impurity in carbon in amounts close to the detectability limit of X-ray diffraction is suspected, but could not be confirmed unambiguously due to the overlap of all strong graphite lines by reflections caused by some of the minerals listed in Table II.

The particular combination of minerals found in carbons tends to indicate a basic high temperature, high pressure intrusive into a more acidic metamorphosed host. There is little doubt that the diamonds were associated for at least part of their history with some type of volcanic activity. The fact that no volcanic pipes have been found so far in Ubangi



could readily be due to the presence of deep layers of sediments of the large lake which covered the entire Ubangi area during the tertiary. Furthermore, the lateritic coverage in central Africa is a considerable obstacle to geological prospection of this area.

## ACKNOWLEDGEMENTS

This investigation was suggested by M. G. Bardet, BRGM, Orleans, France, and would not have been possible without the kind collaboration of Diamond Distributors, Inc. (New York, N.Y.) who donated the specimens. Particular thanks are due B. Jolis and L. R. Kagan for helpful discussions. We also wish to gratefully acknowledge the assistance of M. D. Coutts (RCA, Princeton, N.J.) for scanning electron microscopy, of G. S. Reddy (E. I. du Pont, Wilmington, Del.) for ESR measurements, and of A. L. Mangelsen (Climax Molybdenum Corp., Golden, Colo.) for part of the X-ray diffraction work.

## REFERENECES

- BARDET, M. G. (1970) *Chronique Mines Rech. Miniere* (in press).
- BRUET, E. (1952) *Le Diamant*. Bibliotheque Scientifique Payot (Paris)
- EVANS, T., AND R. PHAAL, (1962) Imperfections in Type I and Type II diamonds. *Proc. Roy. Soc. A*, **270**, 538-552.
- KEH, A. S. (1960) *Direct Observation of Lattice Defects in Crystals*. Interscience Publishers, Inc., New York, 213.
- MEARS, W. H., AND R. F. BOWMAN, (1966) *Indust. Diamond Assoc. Amer., Proc. Tech. Sess. March 7, 1966, Boca Raton, Florida*.
- TRUEB, L. F., AND W. C. BUTTERMAN, (1969) Carbonado, a microstructural study. *Amer. Mineral.* **54**, 412-425.
- , AND E. C. DE WYS (1969) Carbonado: Natural polycrystalline diamond. *Science* **165**, 799-802.

*Manuscript received, January 21, 1971; accepted for publication February 1, 1971.*